

# Measurements in bulk magnetic materials

Fausto Fiorillo

Istituto Nazionale di Ricerca Metrologica-INRIM, Torino, Italy

## Introduction

This lecture will provide an introduction to a few important methods employed in the investigation of intrinsic and technical properties of magnetic materials. We shall treat in particular the following topics: 1) Generation of intense magnetic fields; 2) Investigation of magnetic structures by neutron diffraction; 3) Measurement of Curie temperature and magnetic anisotropy. 4) DC and broadband measurements of soft magnets; 5) Characterization of permanent magnets.

## High fields

Magnetic fields are in most cases generated by means of air-cored windings (solenoids, Helmholtz coils, etc.), but, due to obvious heating problems, the maximum available flux density in water-cooled windings is of the order of 0.1 T. There are two ways to generate higher fields in steady fashion: a) by use of an electromagnet or a permanent magnet; b) by means of a superconducting solenoid. With magnets one can reach a maximum field around 2.5 T. Much stronger fields are obtained using either NbTi ( $B_{\max} \sim 9$  T) or Nb<sub>3</sub>Sn ( $B_{\max} \sim 20$  T) superconducting wires. Even higher field strengths (up to about 30 T) are obtained by the resistive Bitter coils, actually a stack of copper disks with forced water cooling, which are available in few laboratories only. Hybrid sources, made combining a Bitter coil with a superconducting solenoid can overcome the 40 T barrier. Pulsed fields, obtained by discharging a capacitor bank in a solenoid, are routinely applied in industry for magnetization and demagnetization of permanent magnets. With stored energy of the order of 10-20 kJ, peak fields around 8 T can be reached. With several megajoule stored energies an order of magnitude increase of the peak field strength can eventually be obtained, the ultimate limit being posed by the mechanical strength of the coil. By a pulsed field source one can achieve in a single shot the initial magnetization curve  $M(H)$  of a hard magnetic compound. By making the second derivative  $d^2M/dH^2$  of the curve, a cusp is observed in correspondence of  $H = H_k$ , the anisotropy field, defined in a uniaxial material as  $H_k = 2K_u / \mu_0 M_s$ . The anisotropy constant  $K_u$  is therefore retrieved, independent of the morphological and structural properties of the test specimen.

## Neutron diffraction

Neutrons have a small magnetic moment, about  $10^{-3}$  Bohr magnetons, and, being electrically neutral, act as penetrating probes and can be usefully exploited in the study of the intrinsic magnetic properties of bulk materials. Neutron diffraction has therefore become the standard technique for the analysis of the atomic-scale

magnetic structure. With a wavelength of the order of 0.1 nm, thermal neutrons can be diffracted by the atomic planes, according to the same Bragg rule describing X-ray diffraction, the nuclei now being the scattering centres. If the scattering ions have a magnetic moment, the amplitude of the diffracted wave will be affected and a magnetic contribution will add to the nuclear scattering. Fig. 1 shows the scheme

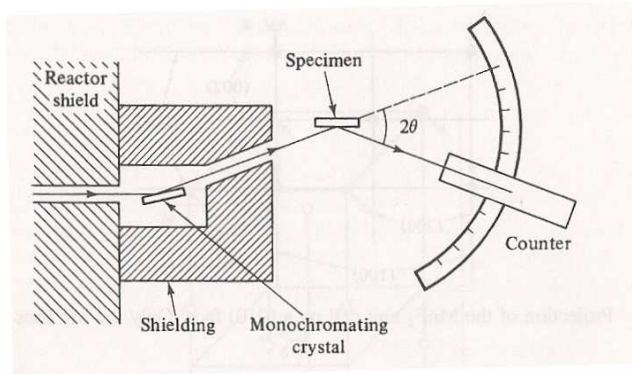


Fig. 1 – Scheme of a neutron diffractometer. The neutron flux of a monochromatic beam obtained by a high-flux reactor is of the order of  $10^{17} \text{ m}^{-2}\text{s}^{-1}$ .

of a neutron diffractometer. Either powder specimens or single crystals are investigated by this technique, which permits one to bring to light the magnetic structure at the atomic scale. Fig. 2 shows, for example, how antiferromagnetic order in the compound  $\text{MnF}_2$  is revealed by the occurrence of a strong 100 superlattice line in the diffraction pattern below the Néel temperature ( $T_N = 67 \text{ K}$ ).

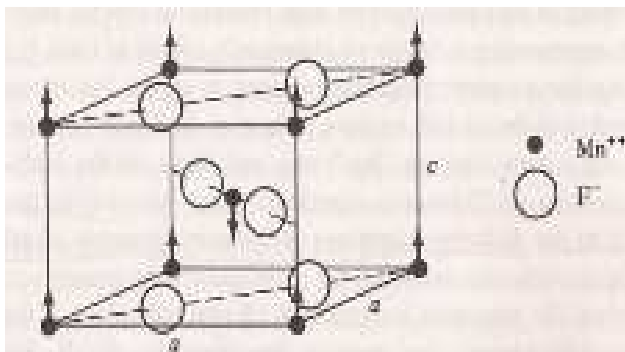
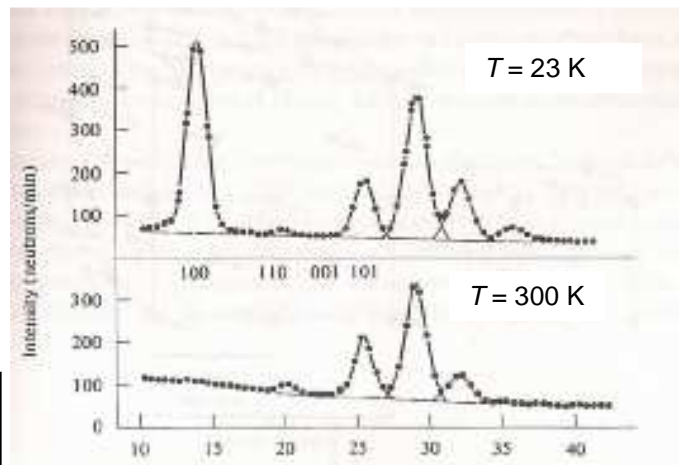


Fig. 2 – Neutron diffraction pattern in  $\text{MnF}_2$ . This compound becomes antiferromagnetic below the Néel temperature  $T_N = 67 \text{ K}$ .



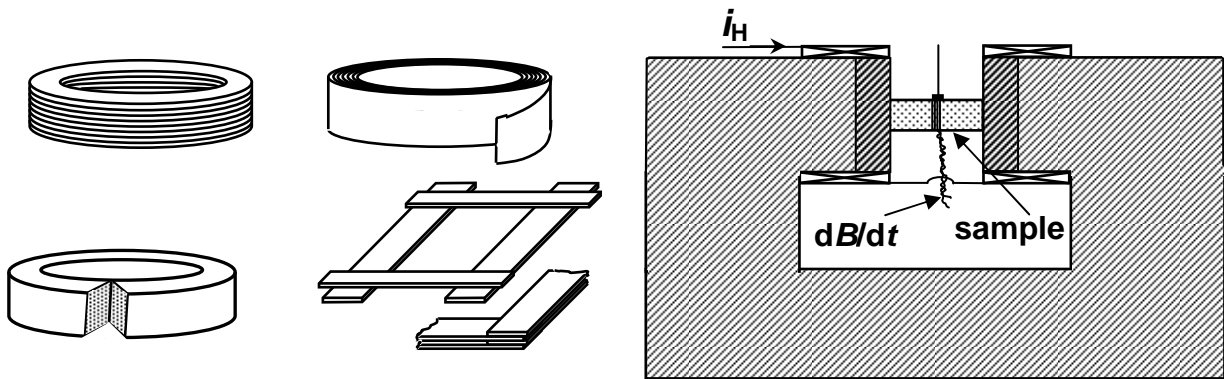
Neutron diffraction experiments can provide, among other things, information on magnetic ordering around the ferromagnetic Curie temperature  $T_{cF}$ , usually distinguishable from the paramagnetic Curie temperature  $T_p$ .  $T_{cF}$  can also be obtained with a number of other methods, including the measurement of the initial susceptibility (Hopkinson’s effect), the isothermal magnetization curves (Arrott plots), the specific heat anomaly by calorimetry.

## Measurements of magnetization curve, hysteresis, and the related parameters

Measuring the magnetization curve of a ferromagnetic material requires either vanishing or accurately known demagnetizing field. The first option is most frequently

required with *fluxmetric* measurements, where the material behaviour is obtained by detecting the flux variation ensuing from the application of a time-varying magnetic field. It is realized (Fig. 3) either by suitably shaping the test specimen or by resorting to a flux-closing yoke, which can also play the role of magnetizer (e.g. an electromagnet). Measurements on open samples are generally of *magnetometric*

Figure 3. How to form a closed magnetic circuit either shaping the sample or using a soft magnetic yoke. The latter method is typically adopted with permanent magnets.



type, where the magnetic moment of a small specimen and its dependence on the applied field strength are determined exploiting the reciprocity principle. Fig. 4, where the sample is assimilated to a point-like magnetic dipole located in the midplane of an Helmholtz pair, provides an illustration of this principle. If the magnetic dipole is in the generic point of coordinates  $(x, y, z)$  and has components  $(m_x, m_y, m_z)$ , the general proportionality relationship between the linked flux  $\Phi_{sm}$  and the magnetic moment  $\mathbf{m}$

$$\Phi_{sm} = \mathbf{k}(x, y, z) \cdot \mathbf{m} = k_x(x, y, z) \cdot m_x + k_y(x, y, z) \cdot m_y + k_z(x, y, z) \cdot m_z,$$

holds, where  $\mathbf{k}(x, y, z)$  is the coil constant. For a magnetic dipole located at the center of a filamentary coil of radius  $R$ , we obtain  $\Phi_{sm} = \mu_0 m / 2R$ . If the search coil is a Helmholtz pair, it is  $\Phi_{sm} = 0.1755 \cdot \mu_0 N m / R$ . The reciprocity principle is exploited in the popular Vibrating Sample Magnetometer (VSM) method, the preferred experimental approach to the DC characterization of thin films and recording media.

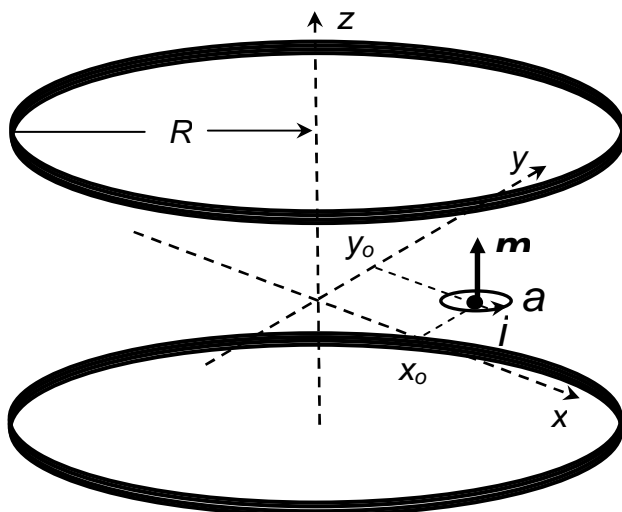


Figure 4. A small sample of magnetic moment  $\mathbf{m}$  is located in the midplane of a Helmholtz pair of radius  $R$ . It is represented as a loop of area  $a$  with a current  $i_m$  flowing in it ( $m = a \cdot i_m$ ). The flux linked with the search coil is  $\Phi = k(x_0, y_0) \cdot m$ , where  $k(x_0, y_0)$  is the value of the coil constant at the loop position. For a moment  $m$  located at the center of the pair, each coil having  $N$  turns, it is  $\Phi = 0.1755 \cdot \mu_0 N m / R$ .

## Measurements in soft magnetic materials

The applications of soft magnets may call for their characterization from DC to microwave frequencies, a feat made difficult by the correspondingly huge dynamic range, possible parasitic effects, and energy dissipation. These problems further compound with the non-linear response of the material. A suitably developed and calibrated fluxmetric device (the hysteresisgraph, Fig. 5) can permit one to achieve broadband characterization of most available soft magnetic materials. When dealing with industrial materials, the necessary requisite of reproducibility is guaranteed by observance of the recognized international measuring standards (for example, the IEC 60404 standards), which call for sinusoidal induction  $B(t)$ . The determination of the  $B(H)$  hysteresis loops versus peak induction and frequency  $f$  is all what is needed for most applications, the property bearing chief technical interest being the magnetic power loss

$$P = f \oint H \cdot dB = f \int_0^T H(t) \cdot \frac{dB(t)}{dt} dt. \quad [\text{W/m}^3]$$

When increasing the testing frequency towards the MHz range, as often required by present-day trends towards device miniaturization, serious limitations arise. They are posed, for example, by the available exciting power, the resolution of the A/D converters, the stray capacitances and inductances, and sample overheating.

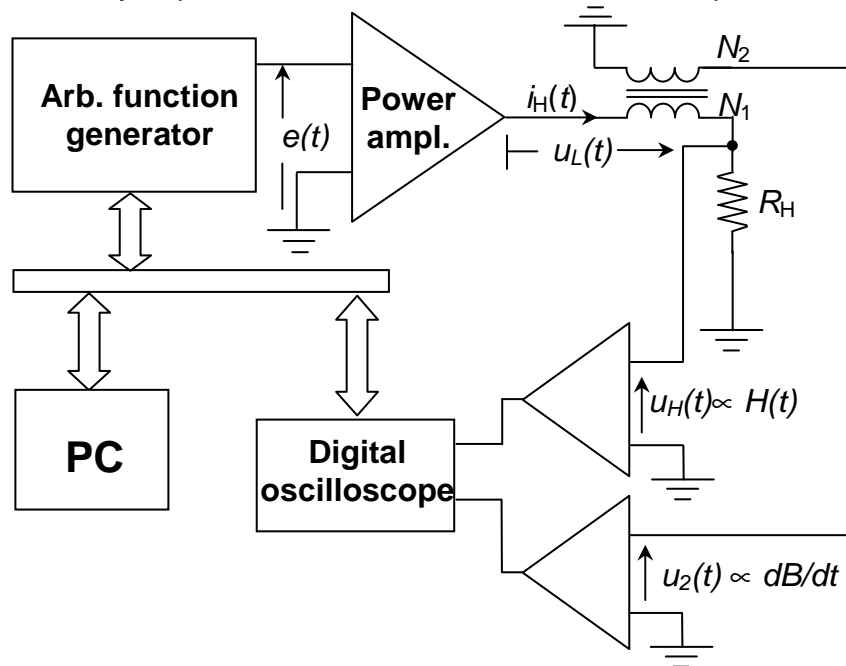


Figure 5. Wattmeter-hysteresisgraph fluxmetric setup implementing digital control by recursive processing of the  $dB/dt$  waveform.

It is then expedient to identify the material behaviour through the complex permeability  $\mu = \mu' - j \mu''$  and its dependence on frequency. This quantity can be obtained up to the natural frequency limit posed either by relaxation losses or ferromagnetic resonance through characterization in a transmission line. In Fig. 6 a ring sample is tested in a coaxial cell by use of a network analyzer. Fig. 7 provides an

example of correspondingly measured broadband (DC – 1GHz) permeability spectrum in a Mn-Zn ferrite, with crossover of  $\mu'$  and  $\mu''$  around the ferromagnetic resonance region.

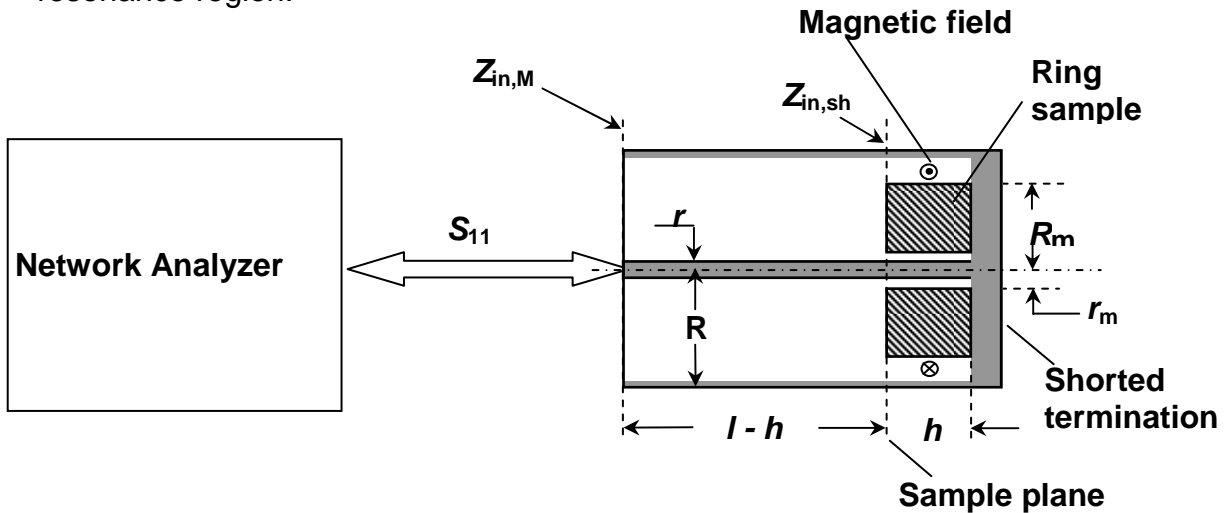


Figure 6. Measurement of the complex permeability of a ring sample and its frequency dependence using the network analyzer. The sample is placed against the shorted termination of a coaxial line and the input impedance at the sample plane  $Z_{in,sh}$ , directly related to the permeability, is obtained by measurement of the reflection coefficient  $S_{11}$ .

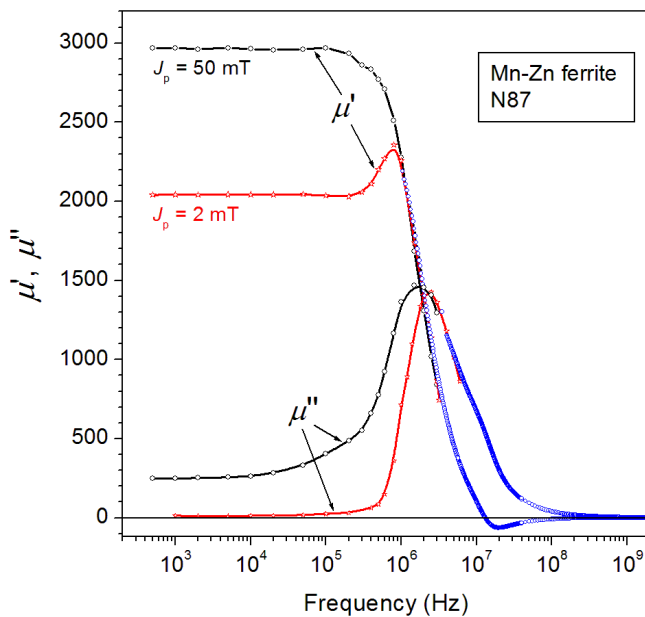


Figure 7. Example of real ( $\mu'$ ) and imaginary ( $\mu''$ ) permeability broadband spectrum measured in a Mn-Zn ferrite ring sample. The occurrence of ferromagnetic resonance is apparent in the behaviour of  $\mu'$ .

### Measurements in permanent magnets

The characterization of permanent magnets is chiefly directed at the determination of those parameters of the hysteresis loop associated with their property of retaining the magnetization and the related energy in the absence of applied fields: remanent magnetization  $J_r$ , coercive fields  $H_{cJ}$  and  $H_{cB}$ , energy product in the second quadrant ( $BH$ ). The high values of the involved field strengths, besides implying a clear distinction between the ( $J, H$ ) and the ( $B, H$ ) curves, makes

manageable the correction for the demagnetizing field and opens the way to both closed-circuit and open-circuit measuring methods. The closed-circuit configuration with electromagnet was schematically shown in Fig.3. Various open-circuit methods are applied in the literature. Testing by the Vibrating Sample Magnetometer (VSM), frequently applied in industry and research, is based on the measurement of the magnetic moment  $m$  of a suitably small specimen by making it to vibrate at the center of a sensing coil assembly. In the example shown in Fig. 8 (transverse vibration) the instantaneous detected signal is  $u(z,t) = m \frac{d}{dz} (k_x(0,0,z)) \cdot \dot{z}$ , where  $k_x$  is the coil constant. Transverse vibration is adopted when the stepwise changing field  $H_a(t)$  is applied by an electromagnet or a permanent magnet source. Longitudinal vibration is adopted with superconducting solenoid sources. Other common open-sample

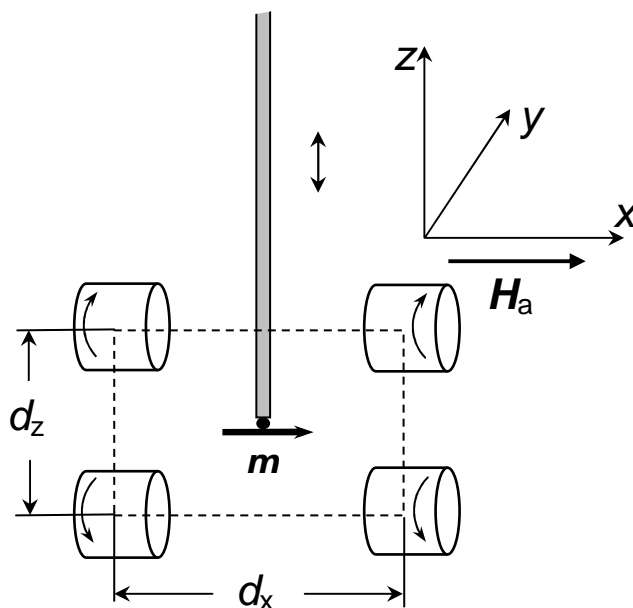


Figure 8. Coil assembly used with perpendicular (z-axis) sample vibration (Mallinson's set). It is usually  $d_z < d_x$ . The arrows marked on the coils identify the way in which the signals from the coils are added. The sample is attached to a non-magnetic vibrating rod.

methods are the Extraction Method and the Alternating Gradient Force Magnetometer. The latter is something of a VSM in reverse, where the coils, supplied by an AC current, are used to generate an alternating field gradient at the sample position. The correspondingly generated force on the sample, proportional to  $m$ , is revealed by a piezoelectric sensor.

## Conclusions

The broad range of properties and operating conditions of magnetic materials require an array of measuring methods, which must satisfy stringent requirements of reproducibility, besides providing solid physical information to fundamental and applied research studies. This lecture will try to convey, under the appropriate physical framework, the basic concepts involved in the realization of present-day measuring systems, aiming at the determination of both intrinsic and technical magnetic properties of the materials.

## References

- [1] T.C. Bacon, *Neutron Diffraction* (Oxford: Clarendon Press) 1975.
- [2] G.I. Squires, *Thermal Neutron Scattering* (New York: Cambridge Univ. Press) 1978.
- [3] H. Zijlstra, *Experimental Methods in magnetism* (Amsterdam: North-Holland) 1967.
- [4] M. McCaig and A.G. Clegg, *Permanent Magnets in Theory and Practice* (London: Pentech Press) 1987.
- [5] E. Steingroever, *Magnetic Measuring Techniques* (Köln: Magnet Physik) 1989.
- [6] P. Lethuillier, *Magnétisme Pratique et Instrumentation*, in *Magnétisme*, vol. II (E. du Trémolet de Lacheisserie, ed., Presses Universitaires de Grenoble, 1999), p. 435.
- [7] F. Fiorillo, *Measurement and Characterization of Magnetic Materials* (Elsevier-Academic Press, Amsterdam) 2004).
- [8] B.D. Cullity and C.D. Graham, *Introduction to Magnetic Materials* (Piscataway, NJ: IEEE Press and Wiley) 2009.
- [9] J.M.D. Coey, *Magnetism and Magnetic Materials* (Cambridge Univ. Press) 2010.
- [10] F. F. Fiorillo, *Measurements of magnetic materials*, *Metrologia*, vol. 47, pp. S114-S142, 2010.
- [11] S. Tumanski, *Handbook of Magnetic Measurements* (CRC Press) 2011.
- [12] BIPM, IEC, IFCC, ISO, IUPAC, IUPAP, OIML, "Guide to the expression of uncertainty in measurement," (International Organization for Standardization, Geneva, Switzerland) 1993.
- [13] BIPM, "Mutual recognition of national measurement standards and of calibration and measurement certificates issued by the national metrology institutes," (Bureau International des Poids et Mesures, Sèvres, 1999); <http://www.bipm.fr/BIPM-KCDB>
- [14] IEC Standard Publications, 60404 Series.